Energetic ion beams near the heliospheric current sheet: Possible evidence for reconnection.

N. Murphy, E.J. Smith, M.E. Burton, D. Winterhalter, all at The Jet Propulsion Laboratory, 4800 Oak Grove Drive, Pasadena, California 91109 and
D.J. McComas, Los Alamos National Laboratory, Los Alamos, New Mexico 87545

Abstract.

Energetic ion data, close to solar wind sector boundaries (the heliospheric current sheet), are examined for the presence of accelerated ions, which may be the signature of magnetic reconnection. Several heliospheric current sheet crossings are found at which such accelerated ions are seen. Two such examples are shown here. The magnetic field and plasma data associated with these events are examined for evidence to support the hypothesis that the observed ions are accelerated by reconnection across the heliospheric current sheet.

Introduction,

Magnetic reconnection is thought to play an important role in heating and accelerating plasmas during magneto spheric substorms, and solar flares. Reconnection is also capable of accelerating a small fraction of the particles in a plasma to superthermal energies, although this acceleration process can be inefficient (Spieser, 1965., Vasyliunas 1980., Mathaeus and Lamkin, 1986.). In both magnetospheric substorms and solar flares there is a basic similarity in the magnetic field geometry; regions of highly sheared, or antiparallel magnetic fields are separated by a current sheet, across which the reconnection takes place, A similar magnetic field configuration can be found in the solar wind, where regions of oppositely directed magnetic fields are separated by the heliospheric current sheet, or sector boundary, Evidence for reconnection in the

component normal to the current sheet, or of the presence of accelerated ions (Levy et al., 1974)

In this work we examine the fluxes of superthermal ions (35 keV - 1.6 Mev) in the vicinity of the heliospheric current sheet. Short duration enhancements are found in the omnidirectional flux of ions with energies less than 150 keV, associated with a plasma sheet region around the heliospheric current sheet (Winterhalter et al., 1991). Examination of the particle distribution in velocity space suggests that these enhancements are caused by the appearance of a low energy ion beam, produced close to the spacecraft. Ions in this energy range are predicted to be produced by magnetic reconnection across the heliospheric current sheet (Goldstein et al., 1986,).

Data Analysis.

The data used in this study were obtained by the ISEE-3 spacecraft when in a halo orbit around the sun-earth libration point L_1. We analyze 24 second resolution magnetic field data from the vector helium magnetometer (Fransden et al., 1978), 24 second resolution plasma data from the Los Alamos plasma instrument (Bame et al., 1978.) and 32 second resolution energetic ion data from the Energetic Proton Anisotropy Spectrometer (EPAS) (Balogh et al., 1978). The EPAS instrument measures the three dimensional energetic ion distribution in the energy range 35 keV < E < 1.6 MeV with a nominal time resolution of 16 seconds. The instrument employs three particle telescopes inclined at 30°, 60° and 135° to the spacecraft spin axis (perpendicular to the ecliptic plane), output from which is binned into 8 azimuthal sectors. There is no discrimination between ion species. Plasma flow data are used to transform the energetic ion distributions measured by the EPAS instrument into the solar wind frame of reference.

Examples.

Figure 1 shows 4 hours of data from 0600 UT to 1000 UT on October 8 1978 (day 281), The top panel displays the omnidirectional ion

flux in the lowest four energy channels of the EPAS instrument with energies 35-56, 56-91, 91-147 and 147-238 keV. The lower three panels show the magnetic field data in spacecraft centered coordinates, where θ is the magnetic field angle out of the ecliptic plane, ϕ is the azimuthal angle, with ϕ = O pointing towards the sun, and |B| is the magnetic field magnitude. Ion data are plotted with a time resolution of 32 seconds while magnetic field data are plotted with 24 seconds resolution.

Prior to 0720 UT ISEE-3 is in a toward magnetic field sector and after 0920 UT the spacecraft is in an away sector. The transition between sectors is accomplished by a rotation in ϕ of $\approx$ 180°, from -45° to 135°. During this period the spacecraft sees two clear encounters with the heliospheric current sheet at 0720 and 0920 UT (marked A and B in the figure) separated by a series of complex rotations in the magnetic field. Throughout, and prior to this period the magnetic field magnitude is depressed, suggesting a plasma sheet structure enclosing the current sheet, Examination of plasma data for this period (not shown) shows that this region contains plasma with an enhanced plasma beta (Winterhalter et al., 1991).

The omnidirectional ion flux is marked by a short ion enhancement, occurring between 0924 and 0930 UT, following the magnetic field rotation, and close to the edge of the plasma sheet. This increase in ion flux is seen clearly in the two lowest energy channels (35-56 and 56-91 keV), and shows a small effect in channel 3 (91 -147 keV), suggesting that there is an energy cutoff somewhere around 150 keV. There is no measurable velocity dispersion seen in the ions which implies a source close to the spacecraft. It should be noted that an energetic ion enhancement is not seen at each current sheet crossing, suggesting a time varying phenomenon.

Figure 2 shows a plot of pitch angle distribution for 32 seconds of data from the 35-56 keV energy channel, centered at 0925:32 UT. The ion flux at small pitch angles increases by more than an order of

magnitude compared to the flux at other pitch angles, suggesting that the increase in omnidirectional flux seen in figure 1 is due to an increased ion flux at pitch angles close to O^{o}.

As an alternative to displaying pitch angle plots, the energetic ion data can be displayed as contour plots in velocity space (velocity parallel and perpendicular to the magnetic field) with contour levels corresponding to differential ion flux in units of $(cm^{2}.s.sr.keV)^{-1}$. Data points are reflected about the parallel velocity axis to produce points with negative perpendicular velocity. This approach allows us to examine the pitch angle and spectral characteristics of the data, over the full energy range of the EPAS instrument. Prior to plotting, the data are transformed into the solar wind frame, using the velocity derived from the Los Alamos plasma instrument on ISEE-3, thus removing the Compton-Getting anisotropy. It should be noted that the contour display of velocity distributions used here relies on producing a regular grid of points from data irregularly spread in velocity space. In the present work this is accomplished by a combination of smoothing and interpolating over the grid, There are several drawbacks of this technique, in particular sharp features in the data are de-emphasized, whilst gaps in data coverage can distort contour lines. These problems can be minimized by superimposing several time frames to produce each plot, although for short duration events this is not always possible. In the present study we have used contour plots made by superimposing two 16 second records, which produces a grid based on 672 points, or four 16 second records producing a grid based on 1344 data points. Notwithstanding the drawbacks mentioned above, we feel that the technique as applied gives a reasonably accurate display of the data for the events studied, although comparison of small scale features of the distributions should be made cautiously.

Shown in figure 3 is a velocity space contour plot of the ion data for the 32 second interval displayed in figure 2, whilst figure 4 shows a contour plot for a 32 second interval centered at 0934:04 UT. The

ion distribution shown in figure 4 is typical of the period surrounding the current sheet crossing and is essentially isotropic. Comparing this to figure 3 we see that at higher energies the distributions are similar, but figure 3 has a low energy beam centered at 3000 km/s (the center velocity of the beam is uncertain, as the enhancement in ion flux may extend below the energy threshold of the EPAS instrument).

A second example is shown in figure 5, which covers 4 hours between 2000 and 2400 UT, again on October 8 1978. The plot organization is the same as figure 1. A crossing of the heliospheric current sheet takes place between 2153 and 2311 UT, during which the magnetic field rotates through 120°, As in the previous example, there is an extended plasma sheet associated with the crossing, having enhanced plasma beta and showing considerable structure in the magnetic field. The omnidirectional energetic ion data show increased fluxes in both 35-56 and 56-91 keV energy channels prior to and during the exit from the plasma sheet at 2311 UT (although the effect seen in the 56-91 keV channel is very small and more localized in time).

Velocity space contour plots are shown in figures 6 and 7, for 64 second intervals centered around 2300:22 and 2336:37 UT, respectively. The first interval is during the ion enhancement, whilst the second occurs 25 minutes after ISEE-3 exits the plasma sheet. The data coverage is different for the two distributions (due to the change in magnetic field orientation), and this could be responsible for the different contour shapes at higher energies. In this example the omnidirectional flux increase is far less pronounced than in the previous case, but the distribution taken during the period of enhanced ion flux (Figure 6) shows a distinct beam at low energies. The distribution taken after the plasma sheet exit (Figure 7) shows no evidence of the beam. In figure 7 we can see that the low energy part of the distribution has a maximum in the perpendicular

direction, suggesting that the low energy ions have a pitch angle distribution peaked at 90°.

The increases in energetic ion flux seen in the above two examples are typical of a number of events seen during the examination of eight days of ion data at heliospheric sector boundaries, In each of the cases an increase in omnidirectional ion flux was caused by the presence of a low energy ion beam in the ion distribution, which was clearly present even when the increase in omnidirectional flux was small.

Although the primary aim of this paper is to report observations of energetic ions associated with the heliospheric current sheet, it is interesting to consider in more detail the magnetic field and plasma observations associated with the events shown. One of the natural consequences of reconnection across the heliospheric current sheet is the production of disconnected loops of magnetic field lines or closed magnetic field loops. Recent observations of electron heat flux dropouts (McComas et al., 1989) have suggested that they occur on magnetic field lines which have been disconnected from the sun by reconnection. Our first example, shown in figure 1, takes place immediately following the onset of one of the heat flux dropouts reported by McComas et al. (The heat flux dropout starts at 0720 UT). The second event presented occurs immediately following a heat flux dropout. In both cases this suggests that we are in a region of the solar wind close to where reconnection has taken place, and may indicate the presence of magnetic field loops which are in the process of being formed. On closer examination of the magnetic field data shown in figure 1 we can see two large bipolar variations in Delta , the magnetic field angle out of the ecliptic plane which are reminiscent of plasmoids in the earth's magnetotail (Hones et al., 1984). Whilst these magnetic field variations could be the signatures of magnetic bubbles produced in the reconnection process, we have not ruled out the possibility that they are caused by some other perturbation of the heliospheric current sheet,

Discussion.

We have presented two examples of heliospheric current sheet crossings in which accelerated ions are seen. Although the acceleration of particles in the vicinity of a simple X-type neutral point is not an efficient process, due to the limited time a particle spends close to the X-point (Spieser, 1965., Vasyliunas 1980,), recent work (Mathaeus and Lamkin, 1986., Goldstein et a]., 1986.) has suggested that the inclusion of turbulence in the dynamics of reconnection can appreciably increase the efficiency of the acceleration process. In particular Goldstein et al. calculate the maximum expected energy of particles accelerated during turbulent reconnection across the heliospheric current sheet, and obtain a value of 100 keV, which is in agreement with the observations presented here. Given the limited number of examples studied to date, we make no attempt to estimate the rate of occurrence of reconnection across the heliospheric current sheet, but if this process is common then it will have a profound effect on the structure of the solar wind. In particular we might expect to see plasmoid-like structures, similar to the ones seen in figure 1, more frequently at larger heliospheric distances. Also, if the heat flux dropouts reported by McComas et al 1989, are caused by the same process, then they will be more common at larger distances from the sun.

Acknowledgments.

Portions of this work were carried out at the Jet propulsion Laboratory, under contract with the National Aeronautics and Space Administration.

References.

Balogh, A., G. van Dijen, J. van Genechten, J. Hem-ion, R.J. Hynds, G. Korfmann, T. Iversen, J. van Rooijen, T. Sanderson, G. Stevens and K.-P. Wenzel, The low energy proton experiment on ISEE-C, IEEE Trans. Geosci. Electron., GE-16, 195, 1978.

Dungey, J. W., Cosmic Electrodynamics, Cambridge University, Cambridge, 1958.

Fransden, A. M. A., B.V. Connor, J. van Amersfoort and E.J. Smith, The ISEE-C Vector Helium Magnetometer, IEEE Trans. Geosci. Electron., GE-16, 195, 1978.

Goldstein, M. L., W.H. Matthaeus and J.J. Ambrosiano, Acceleration of charged particles in magnetic reconnection: Solar flares, the magnetosphere, and solar wind, Geophys. Res. Lett. 13, 3 p205 1986.

Hones, E, W., Jr., D.N. Baker, S.J. Bame, W.C. Feldman, J.T. Gosling, D.J. McComas, R.D. Zwickl, J.A. Slavin, E.J. Smith, and B.T. Tsurutani, Structure of the magnetotail at 220 R_E , and its response to geomagnetic activity, J. Geophys. Res., 11, 5, 1984.

Levy, E. H., F.M. Ipavich and G. Gloeckler, Possible acceleration of charged particles through the reconnection of magnetic field lines in interplanetary space. Geophys. Res, Lett. 1, 4 p1 45 1974.

Mathaeus, W. H., S.L. Lamkin, Turbulent magnetic reconnection, Phys. Fluids Vol 29 No 8, 1986

McComas, D. J., J.T. Gosling, J.L. Phillips and S.J. Bame, Electron heat flux dropouts in the solar wind: Evidence for interplanetary field line reconnection, J. Geophys. Res., 94, 6907, 1989.

Speiser, T. W., Particle trajectories in model current sheets, 1, Analytical solutions, J. Geophys. Res., 70, 4219, 1965.

Vasyliunas, V. M., Upper limits on the electric field along a magnetic O line, J. Geophys. Res. 85, 4616, 1980.

Winterhalter, D. W., E.J. Smith, N. Murphy and M.E. Burton, The heliospheric plasma sheet. To be submitted to J. Geophys. Res., 1991.

Figure captions.

Figure 1.
Energetic ion and magnetic field data for a four hour period between 0600 and 1000 UT on October 8 1978. The top panel shows the omnidirectional ion flux in the 35-56, 56-91, 91-147 and 147-238 keV energy channels. The lower three panels show the magnetic field magnitude, in nT, the azimuthal magnetic field angle ϕ, with 0° towards the sun, and the angle of the magnetic field out of the ecliptic plane, (3.

Figure 2.
Differential flux plotted against pitch angle for a superposition of two 16 second records centered at 0925:32 UT on 'October 8 1978.

Figure 3.
Contour plot of differential flux in velocity space for a 32 second period centered at 0925:32 UT on October 8 1978. Contours are spaced geometrically, with the lowest being at .25 $(cm^2.s.sr.keV)^{-1}$.

Figure 4.
As for figure 3 for a 32 second period centered at 0934:04 UT on October 8 1978.

Figure 5.
As for figure 1 for a four hour period between 2000 and 2400 UT on October 8 1978.

Figure 6.
As for figure 3 for a 64 second interval centered at 2300:22 UT on October 8 1978.

Figure 7.
As for figure 3 for a 64 second interval centered at 2336:37 UT on October 8 1978.

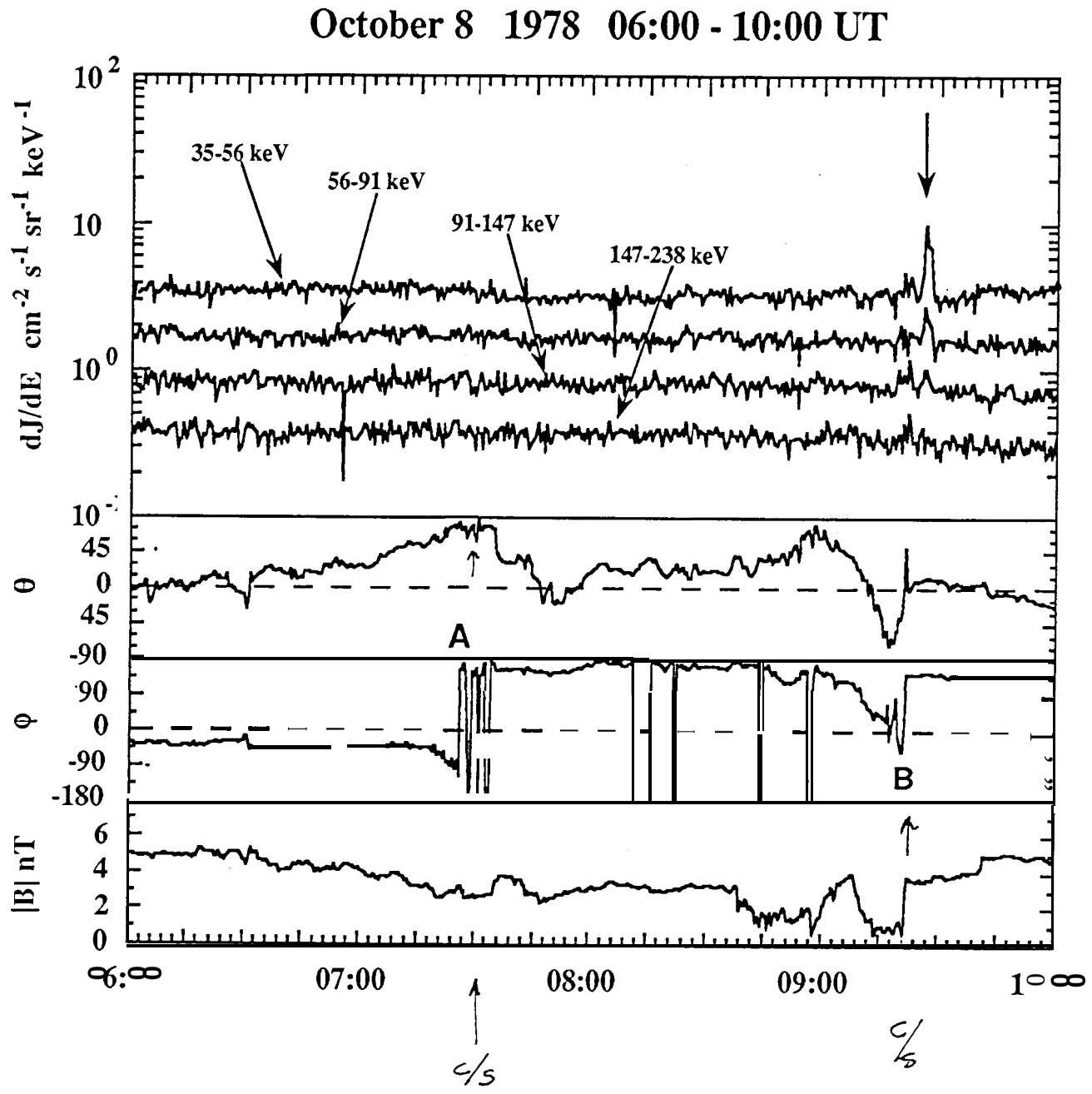
October 8 1978 06:00 - 10:00 UT
dJ/dE cm-2 s-1 sr-1 keV-1
35-56 keV
56-91 keV
91-147 keV
147-238 keV
θ
φ
A
B
|B| nT
06:00
07:00
08:00
09:00
10:00
C/S
C/S

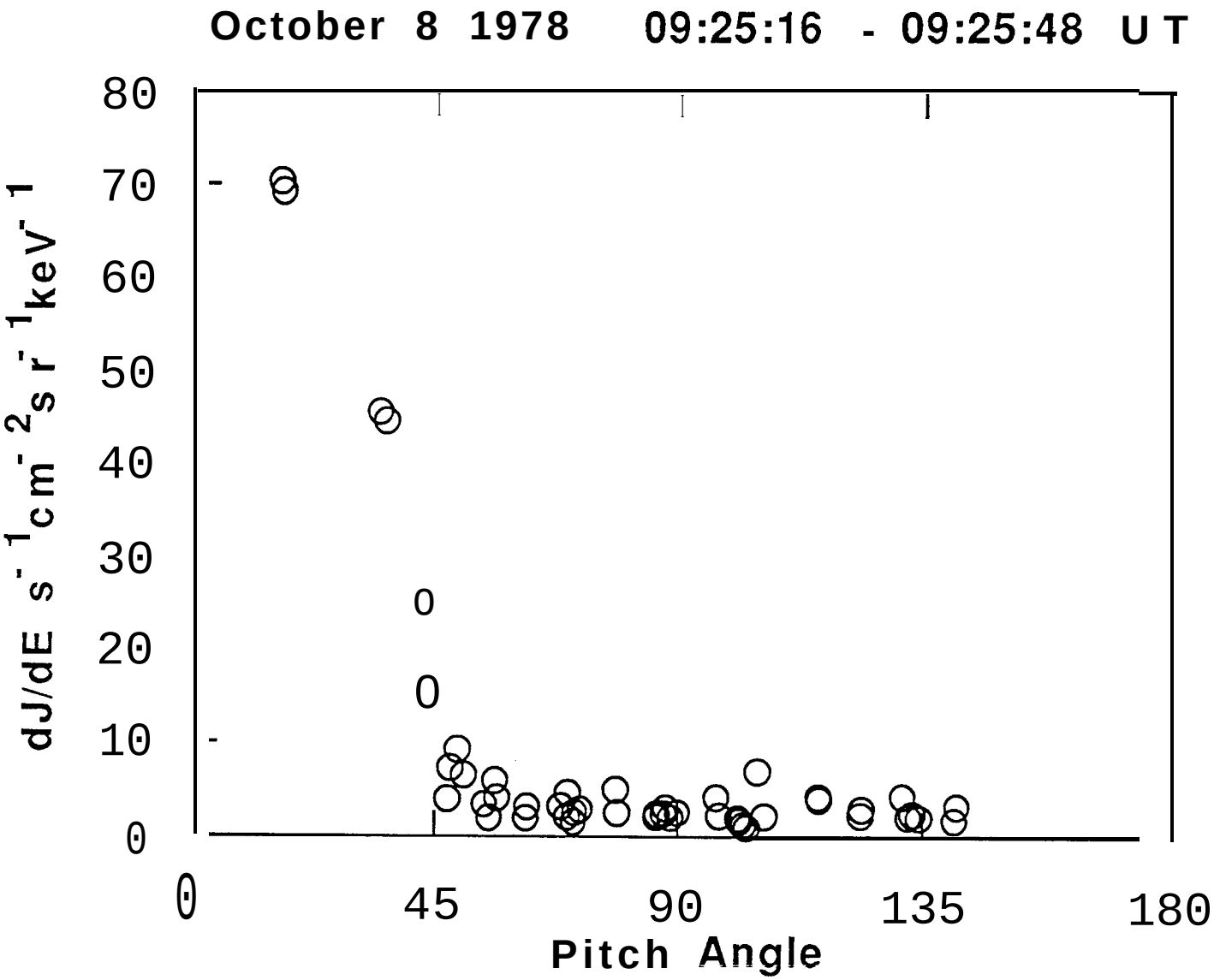
October 8 1978 09:25:16 - 09:25:48 U T
dJ/dE s⁻¹cm⁻²sr⁻¹keV⁻¹
80
70
60
50
40
30
20
10
0
0
45
90
135
180
Pitch Angle

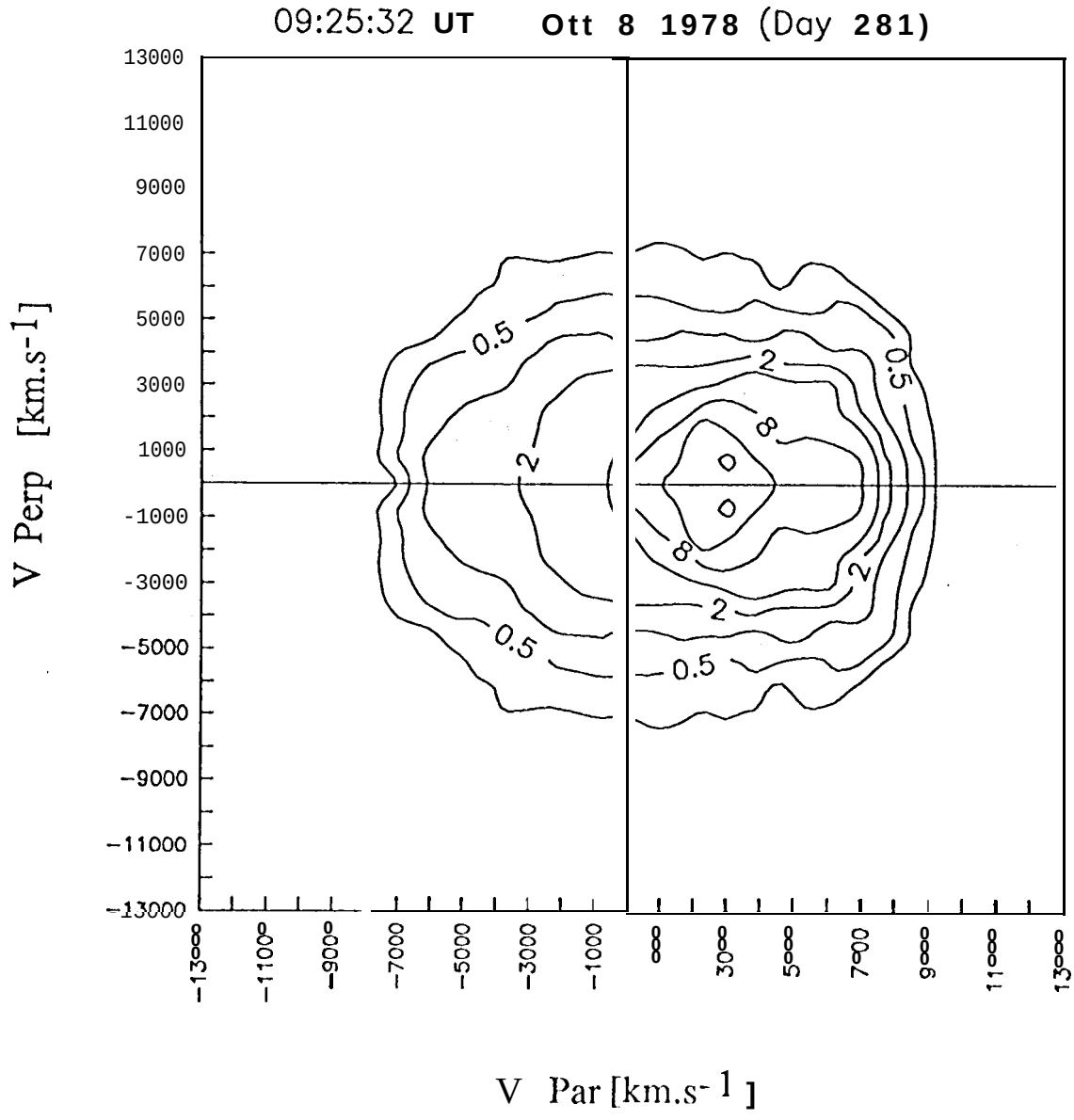
09:25:32 UT Ott 8 1978 (Day 281)
V Perp [km.s-1]
V Par [km.s-1]
13000
11000
9000
7000
5000
3000
1000
-1000
-3000
-5000
-7000
-9000
-11000
-13000
0.5
2
8
0

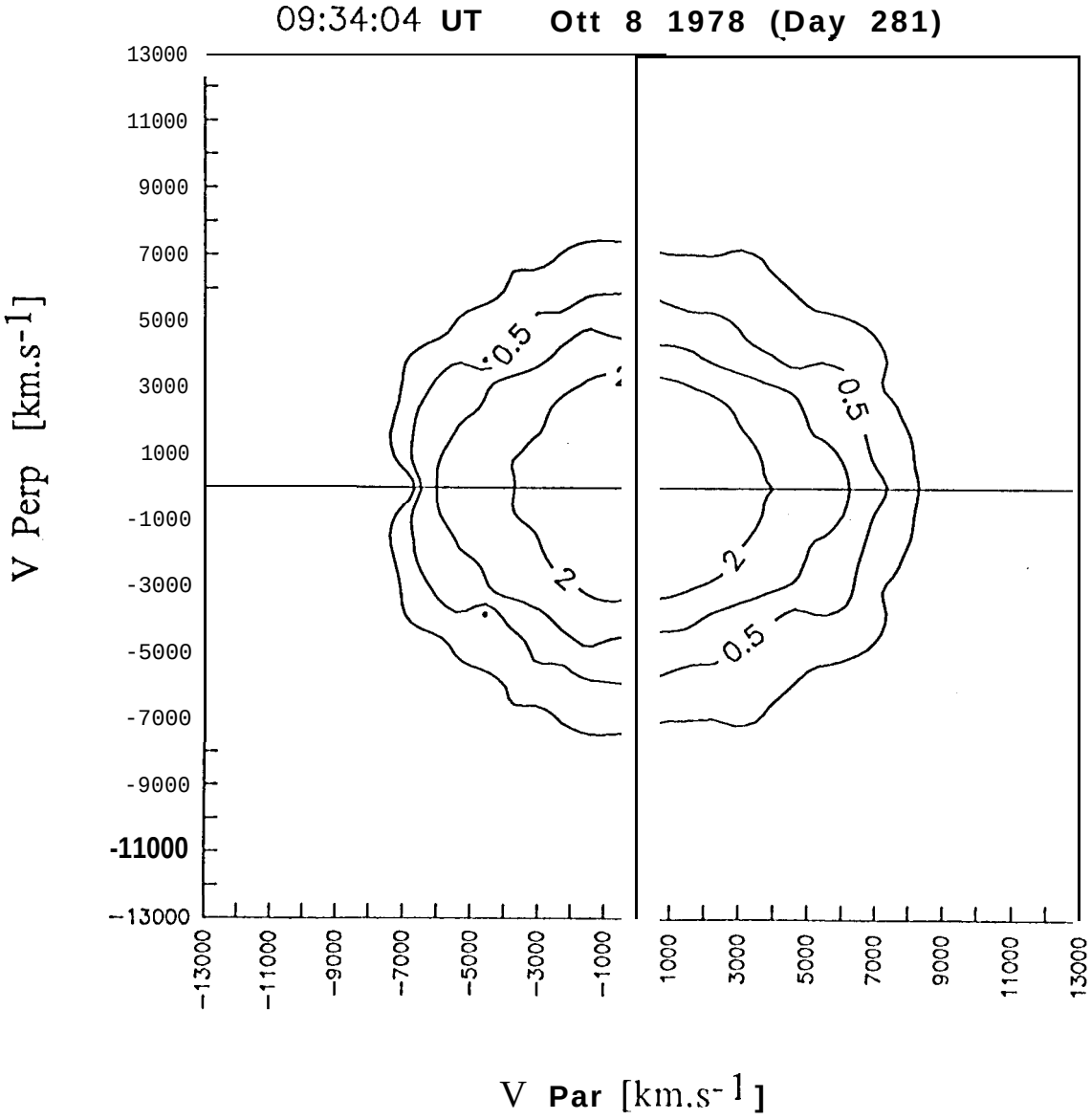
09:34:04 UT Ott 8 1978 (Day 281)
13000
11000
9000
7000
5000
3000
1000
-1000
-3000
-5000
-7000
-9000
-11000
-13000
V Perp [km.s-1]
0.5
2
0.5
2
0.5
-13000
-11000
-9000
-7000
-5000
-3000
-1000
1000
3000
5000
7000
9000
11000
13000
V Par [km.s-1]

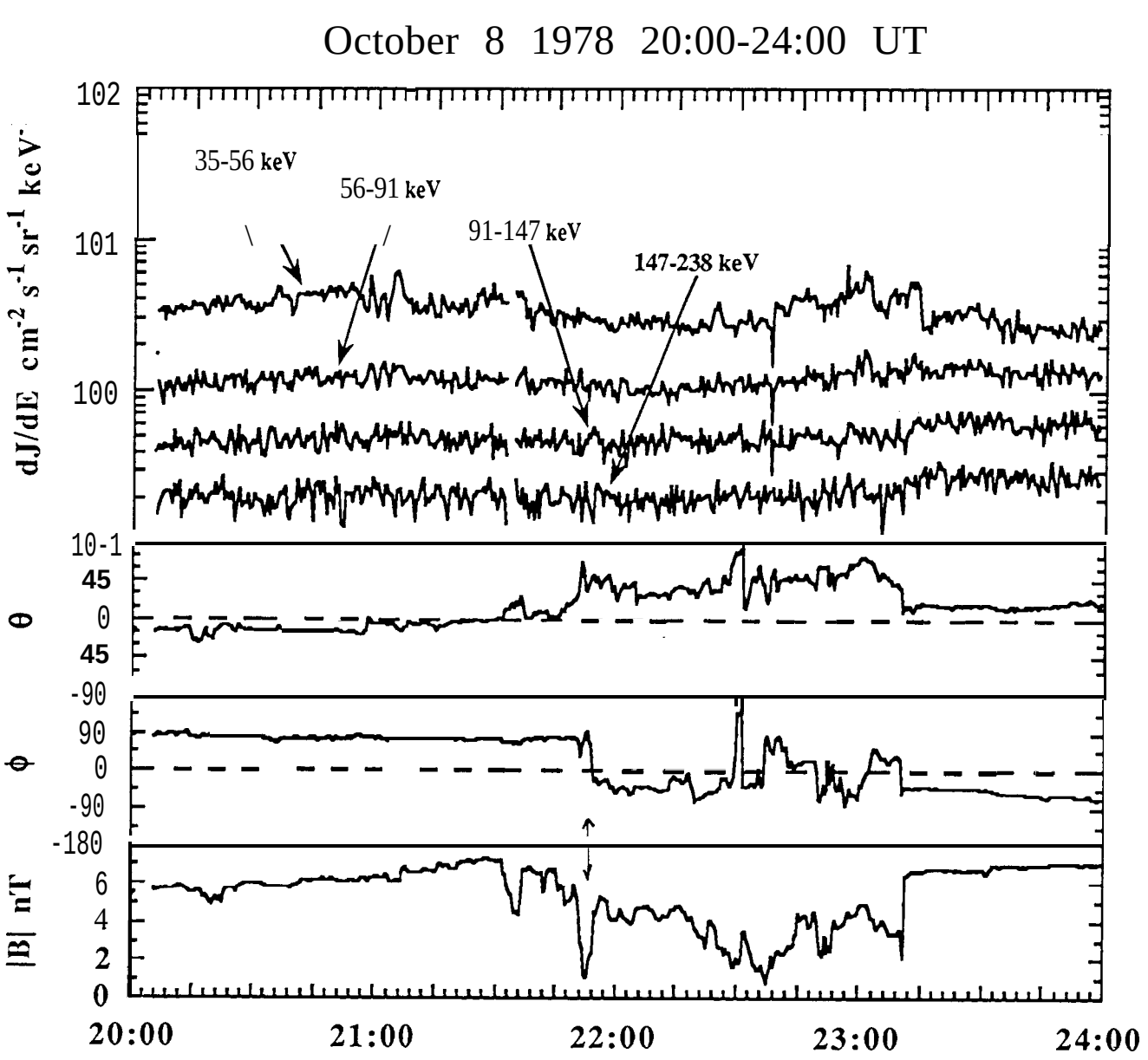
October 8 1978 20:00-24:00 UT
102
101
100
35-56 keV
56-91 keV
91-147 keV
147-238 keV
dJ/dE cm-2 s-1 sr-1 keV-
10-1
45
0
45
θ
-90
90
0
-90
-180
φ
6
4
2
0
|B| nT
20:00
21:00
22:00
23:00
24:00

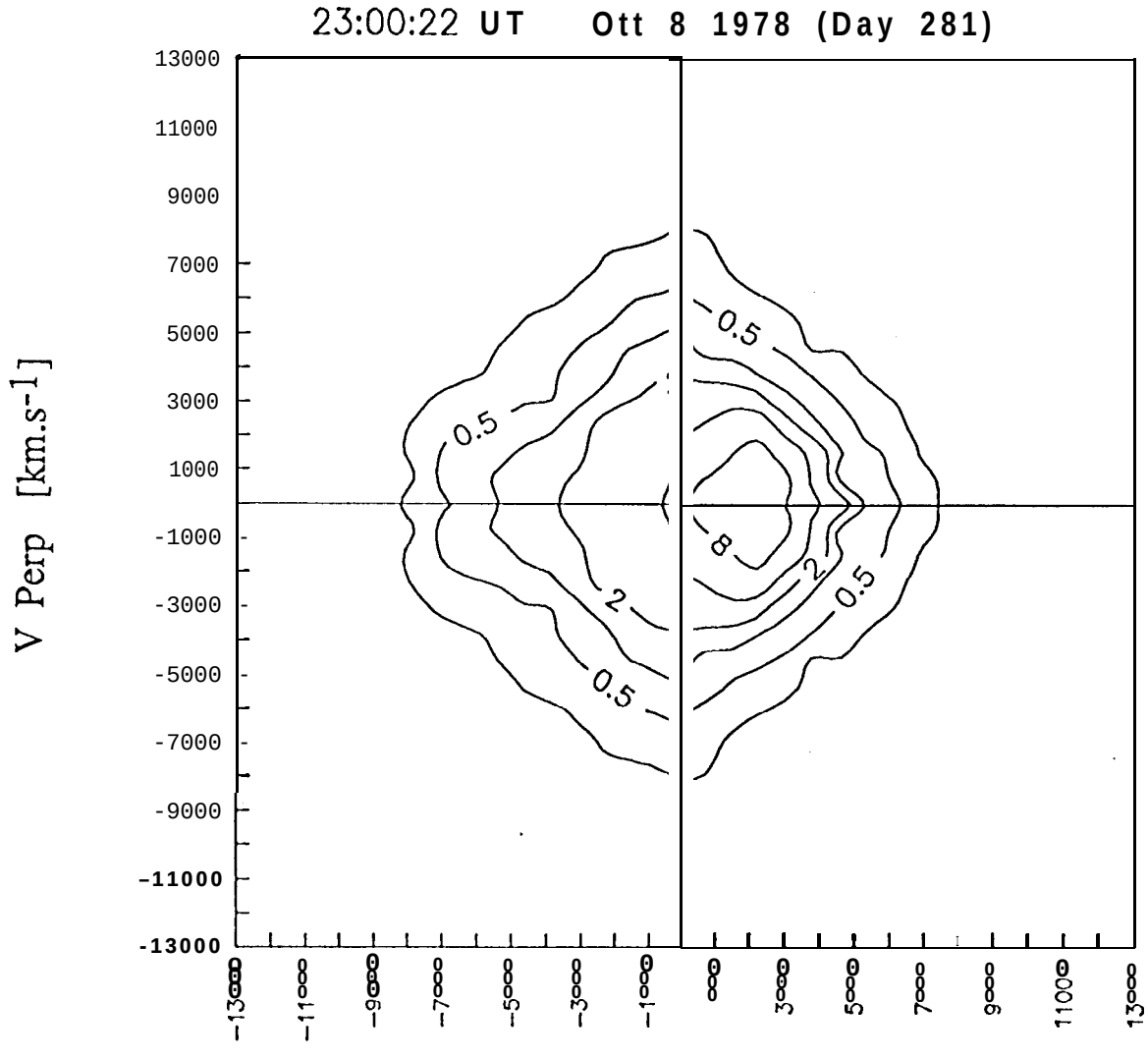
23:00:22 UT Ott 8 1978 (Day 281)
13000
11000
9000
7000
5000
3000
1000
-1000
-3000
-5000
-7000
-9000
-11000
-13000
0.5
0.5
2
0.5
8
2
0.5
V Perp [km.s-1]
V Par [km.s-1]

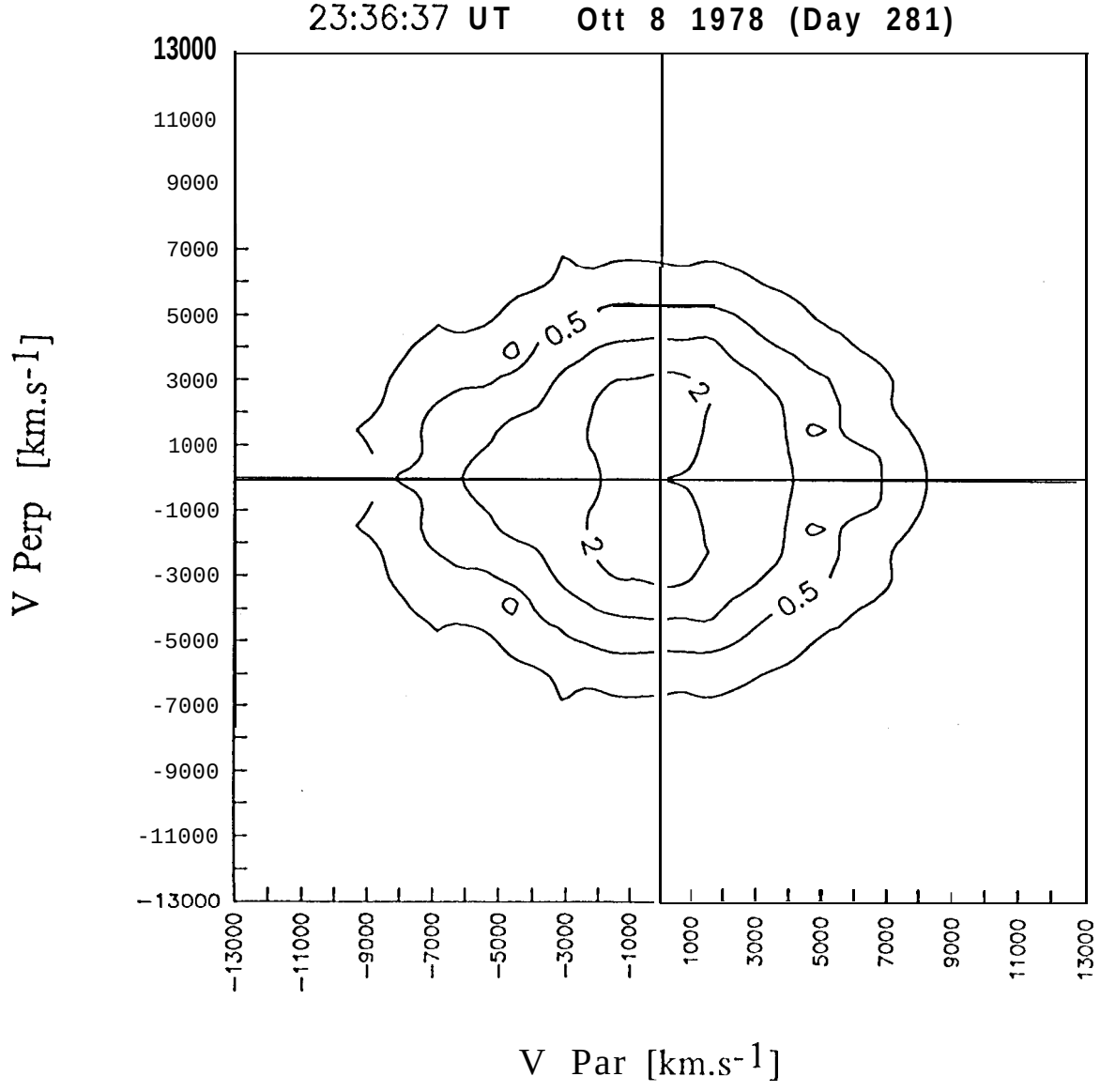
23:36:37 UT Ott 8 1978 (Day 281)
13000
11000
9000
7000
5000
3000
1000
-1000
-3000
-5000
-7000
-9000
-11000
-13000
V Perp [km.s-1]
0
0.5
1
2
-13000
-11000
-9000
-7000
-5000
-3000
-1000
1000
3000
5000
7000
9000
11000
13000
V Par [km.s-1]